Int. J. Solids Structures Vol. 28, No. 1, pp. 105–113, 1991
Printed in Great Britain.

0020-7683/91 $3.00 + .00

THE FREE-EDGE STRESS SINGULARITY AT AN INTERFACE BETWEEN BILINEAR MATERIALS

C. CHUNG† and J. W. EISCHEN
Department of Mechanical and Aerospace Engineering, North Carolina State University, Raleigh, NC 27695-7910, U.S.A.

(*Received* 2 *April* 1990; *in revised form* 16 *August* 1990)

Abstract—The degree of the stress singularity that occurs at the termination of an interface between materials exhibiting bilinear stress–strain response under plane strain conditions is calculated. The governing elasticity equations together with traction-free boundary conditions and interface continuity conditions define a two-point boundary value problem. The stress components near the free edge are assumed to be proportional to r^{s-1}, with solutions existing only for certain values of s. Finding these values entails the solution of a generalized eigenvalue problem. Because it has been impossible to integrate the differential equations analytically, the integration has been performed numerically with a shooting method coupled with a Newton improvement scheme.

INTRODUCTION

It has long been known that the stresses along a bimaterial interface become singular when the interface terminates at a traction-free edge. Many investigators have presented stress singularity calculations for these types of structures for linear elastic materials (Bogy, 1968, 1970, 1971; Hein and Erdogan, 1971; Dundurs, 1969). Bogy (1968) considered the plane problem of two dissimilar orthogonal elastic wedges, bonded together and subjected to surface traction on the boundary. With the aid of the Mellin transform in conjunction with the Airy stress function, the solution of the transformed problem is obtained. The asymptotic behavior of the elastic solution in the vicinity of the intersection of the bonded and loaded planes was investigated. Certain components of stress along the interface were found to be singular. Bogy (1970) elaborated on his earlier study after a discussion by Dundurs (1969) revealed a systematic way of parameterizing the results. Bogy (1971) investigated the much more general problem of bonded dissimilar elastic wedges with arbitrary wedge angles. The emphasis here was placed on the investigation of the dependence of the order of singularity in the stress field at the apex of the wedge on the wedge angle and material constants. Dempsey and Sinclair (1981) provide analytical information on the stress which can occur in the vicinity of the vertex of a two-dimensional wedge for a wide range of boundary and interface conditions. In a recent paper, Duva (1988) employed an idealized model of a fiber end consisting of an orthogonal rigid wedge embedded in a nonlinear material to investigate the singular behavior of the stress and strain fields at the corner of a fiber.

The purpose of the present paper is to extend Duva's work to the case of a bimaterial interface problem where each material is assumed to have a bilinear stress-strain response. Specifically, the degree of stress singularity that occurs at the free edge in a bimaterial strip under plane strain conditions is sought. The governing elasticity equations together with the traction-free boundary conditions and the interface continuity conditions define a two-point boundary value problem. The solution results in a generalized eigenvalue problem where the degree of the stress singularity is the eigenvalue. Because it has been impossible to integrate the governing differential equations analytically, their integration has been performed numerically. The investigation carried out in this paper was focused on stress components proportional to r^{s-1}, r being the distance from the point at which the singularity occurs, and $0 < s < 1$.

Specific numerical results are presented for material combinations that occur frequently in microelectronic applications.

† Presently at Korea Atomic Energy Institute, PO Box 7, Daeduk-Danji, Taejeon, Korea 305-353.

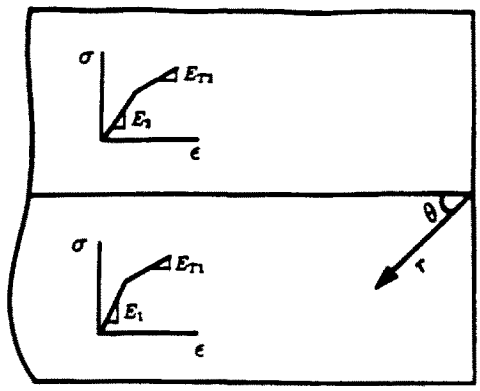

Fig. 1. Configuration of bimaterial interface.

FORMULATION

The physical configuration under investigation consists of two layers joined by a perfect bond. Figure 1 is a schematic of the bimaterial strip. A local polar coordinate system has been erected at the point of anticipated stress singularity.

The stress equilibrium equations relative to this coordinate system are

$$\frac{\partial(r\sigma_{rr})}{\partial r} + \frac{\partial \sigma_{r\theta}}{\partial \theta} - \sigma_{\theta\theta} = 0 \tag{1}$$

$$\frac{\partial(r\sigma_{r\theta})}{\partial r} + \frac{\partial \sigma_{\theta\theta}}{\partial \theta} + \sigma_{r\theta} = 0 \tag{2}$$

and the linear strain–displacement equations are

$$\varepsilon_{rr} = \frac{\partial u}{\partial r} \tag{3}$$

$$\varepsilon_{\theta\theta} = \frac{1}{r}\frac{\partial v}{\partial \theta} + \frac{u}{r} \tag{4}$$

$$\varepsilon_{r\theta} = \frac{1}{2}\left(\frac{1}{r}\frac{\partial u}{\partial \theta} + \frac{\partial v}{\partial r} - \frac{v}{r}\right). \tag{5}$$

Here u and v are the radial and tangential components of displacement, respectively. Note that linear strain–displacement equations are used even though large strains are anticipated near $r = 0$. This is a convenient simplification that has been taken advantage of in many earlier investigations of related problems [e.g. Hutchinson (1968)].

The uniaxial stress–strain relationship for the material in each layer is assumed to obey the following nonlinear elastic-plastic response (see Fig. 1)

$$\varepsilon = \frac{\sigma}{E} \quad \sigma < \sigma_0 \tag{6}$$

$$\varepsilon = \varepsilon_0 + \frac{\sigma - \sigma_0}{E_T} \quad \sigma > \sigma_0, \tag{7}$$

where E and E_T are the elastic modulus and the "so-called" tangent modulus of the material, respectively. The symbols σ_0 and ε_0 ($\varepsilon_0 = \sigma_0/E$) represent constants that can be interpreted loosely as yield stress and strain, respectively. This equation is strictly applicable for a

monotonically increasing stress and cannot accommodate elastic unloading. Alternatively, eqn (7) can be viewed as describing a nonlinear elastic material. This will be the viewpoint adopted in this paper. The multiaxial isotropic generalization is

$$\varepsilon_{ij} = \frac{1}{E}\left[(1+\nu)\sigma_{ij} - \nu\delta_{ij}\sigma_{kk} + \frac{3}{2}\left(\frac{E}{E_T} - 1\right)\frac{\sigma_e - \sigma_0}{\sigma_e} s_{ij}\right] \quad \text{for } \sigma_e > \sigma_0, \tag{8}$$

where s_{ij} is the deviatoric stress defined by $s_{ij} = \sigma_{ij} - \frac{1}{3}\sigma_{kk}\delta_{ij}$. The symbol σ_e represents the effective stress defined by $\sigma_e = (\frac{3}{2}s_{kl}s_{kl})^{1/2}$. Here ν is Poisson's ratio. We will assume that in the vicinity of the traction-free edge, stresses are sufficiently high that eqn (8) holds. The first two terms in the brackets of eqn (8) describe the usual linear elastic behavior whereas the third term contains the tangent modulus that produces the plastic (or nonlinear elastic) response. If the material is regarded as a deformation theory material, the initial elastic portion of the strain must be retained. The elastic component of the strain does not become negligible compared to the plastic strain for large stresses. Note that only the plastic component of the strain is necessarily incompressible.

For the displacement and stress field near the point $r = 0$, a separation of variables solution is proposed in the form following Ponte Castañeda (1987)

$$u_l = \bar{K} r^s f_{1l}(\theta), \quad v_l = \bar{K} r^s f_{2l}(\theta), \tag{9}$$

$$\sigma_{\theta\theta l} = E_l \bar{K} r^{s-1} f_{3l}(\theta), \quad \sigma_{r\theta l} = E_l \bar{K} r^{s-1} f_{4l}(\theta), \tag{10}$$

$$\sigma_{rrl} = E_l \bar{K} r^{s-1} f_{5l}(\theta), \quad \sigma_{zzl} = E_l \bar{K} r^{s-1} f_{6l}(\theta), \tag{11}$$

where the $f_{il}(\theta)$, $i = 1, 2, \ldots, 6$ are as yet undetermined functions of θ. The subscript l takes on the values $l = 1, 2$ depending on which layer is considered. The constant $E_l\bar{K}$ has been included, $\bar{K}$ having the dimension of $(length)^{1-s}$, to render f_{il} dimensionless. These general formulas for displacement and stress lead to four coupled first-order ordinary differential equations and two algebraic equations in each layer.

Layer 1

If the equation for ε_{rr} is formed using eqn (3) and eqn (8), the following algebraic equation is obtained

$$sf_{11} = f_{51} - \nu_1(f_{31} + f_{61}) + \frac{A_1}{3}(2f_{51} - f_{31} - f_{61}). \tag{12}$$

Then if the condition $\varepsilon_{zz} = 0$ (plane strain) is enforced with eqn (8), another algebraic equation is obtained,

$$f_{61} - \nu_1(f_{51} + f_{31}) + \frac{A_1}{3}(2f_{61} - f_{51} - f_{31}) = 0. \tag{13}$$

Next, the stresses given by eqns (10)-(11) are substituted into the equilibrium equations. Two differential equations result,

$$sf_{51} + f'_{41} - f_{31} = 0 \tag{14}$$

$$(s+1)f_{41} + f'_{31} = 0 \tag{15}$$

where the superscript prime $'$ indicates ordinary differentiation with respect to θ. Finally, the equations for $\varepsilon_{\theta\theta}$ and $\varepsilon_{r\theta}$ are formed using eqn (4) and eqn (5) in eqn (8), with two additional differential equations resulting,

$$f'_{21}+f_{11}=f_{31}-\nu_1(f_{51}+f_{61})+\frac{A_1}{3}(2f_{31}-f_{51}-f_{61}) \tag{16}$$

$$\tfrac{1}{2}[f'_{11}+(s-1)f_{21}]=f_{41}(1+\nu_1+A_1). \tag{17}$$

Layer 2

A similar set of differential algebraic equations is obtained for Layer 2:

$$sf_{12}=f_{52}-\nu_2(f_{32}+f_{62})+\frac{A_2}{3}(2f_{52}-f_{32}-f_{62}) \tag{18}$$

$$f_{62}-\nu_2(f_{52}+f_{32})+\frac{A_2}{3}(2f_{62}-f_{52}-f_{32})=0 \tag{19}$$

$$sf_{52}+f'_{42}-f_{32}=0 \tag{20}$$

$$(s+1)f_{42}+f'_{32}=0 \tag{21}$$

$$f'_{22}+f_{12}=f_{32}-\nu_2(f_{52}+f_{62})+\frac{A_2}{3}(2f_{32}-f_{52}-f_{62}) \tag{22}$$

$$\tfrac{1}{2}[f'_{12}+(s-1)f_{22}]=f_{42}(1+\nu_2+A_2). \tag{23}$$

The constants A_1 and A_2 appearing in the equations above are

$$A_l=\frac{3}{2}(\alpha_l-1)\left(\frac{\sigma_{el}-\sigma_{0l}}{\sigma_{el}}\right) \quad \text{where} \quad \alpha_l=\frac{E_{Tl}}{E_l}. \tag{24}$$

Assuming that the stresses are large near the singularity, $((\sigma_{el}-\sigma_{0l})/\sigma_{el})\to 1$. Thus, this term is omitted in subsequent computations for A_l. The functions $f_{5l}(\theta)$ and $f_{6l}(\theta)$ can be eliminated solving eqns (12)–(13) or eqns (18)–(19) simultaneously,

$$f_{5l}=\frac{1}{\Delta}\left[\left(\nu_l+\frac{A_l}{3}\right)(1+\nu_l+A_l)f_{3l}+\left(1+\frac{2}{3}A_l\right)sf_{1l}\right] \tag{25}$$

$$f_{6l}=\frac{1}{\Delta}\left[\left(\nu_l+\frac{A_l}{3}\right)(1+\nu_l+A_l)f_{3l}+\left(\nu_l+\frac{1}{3}A_l\right)sf_{1l}\right] \tag{26}$$

where $\Delta=(1+\frac{2}{3}A_l)^2-(\nu_l+\frac{1}{3}A_l)^2$.

With these results the 12 differential algebraic equations are effectively reduced to a system of eight first-order differential equations

$$f'_{11}=2f_{41}(1+\nu_1+A_1)-(s-1)f_{21} \tag{27}$$

$$f'_{21}=f_{31}-\nu_1(f_{51}+f_{61})+\frac{A_1}{3}(2f_{31}-f_{51}-f_{61})-f_{11} \tag{28}$$

$$f'_{31}=-(s+1)f_{41} \tag{29}$$

$$f'_{41}=f_{31}-sf_{51} \tag{30}$$

$$f'_{12}=2f_{42}(1+\nu_2+A_2)-(s-1)f_{22} \tag{31}$$

$$f'_{22} = f_{32} - \nu_2(f_{52}+f_{62}) + \frac{A_2}{3}(2f_{32}-f_{52}-f_{62}) - f_{12} \tag{32}$$

$$f'_{32} = -(s+1)f_{42} \tag{33}$$

$$f'_{42} = f_{32} - sf_{52}. \tag{34}$$

What remains is to specify the traction-free edge conditions and the interface continuity conditions. Referring to Fig. 1, the traction-free edge conditions are:

Layer 1

$$\sigma_{\theta\theta 1}\left(r, \theta = \frac{\pi}{2}\right) = 0 \quad \Rightarrow \quad f_{31}\left(\frac{\pi}{2}\right) = 0 \tag{35}$$

$$\sigma_{r\theta 1}\left(r, \theta = \frac{\pi}{2}\right) = 0 \quad \Rightarrow \quad f_{41}\left(\frac{\pi}{2}\right) = 0 \tag{36}$$

Layer 2

$$\sigma_{\theta\theta 2}\left(r, \theta = -\frac{\pi}{2}\right) = 0 \quad \Rightarrow \quad f_{32}\left(-\frac{\pi}{2}\right) = 0 \tag{37}$$

$$\sigma_{r\theta 2}\left(r, \theta = -\frac{\pi}{2}\right) = 0 \quad \Rightarrow \quad f_{42}\left(-\frac{\pi}{2}\right) = 0. \tag{38}$$

The following equations enforce continuity of traction and displacement along the interface:

$$\sigma_{\theta\theta 1}(r, \theta = 0) = \sigma_{\theta\theta 2}(r, \theta = 0) \quad \Rightarrow \quad E_1 f_{31}(0) = E_2 f_{32}(0) \tag{39}$$

$$\sigma_{r\theta 1}(r, \theta = 0) = \sigma_{r\theta 2}(r, \theta = 0) \quad \Rightarrow \quad E_1 f_{41}(0) = E_2 f_{42}(0) \tag{40}$$

$$u_1(r, \theta = 0) = u_2(r, \theta = 0) \quad \Rightarrow \quad f_{11}(0) = f_{12}(0) \tag{41}$$

$$v_1(r, \theta = 0) = v_2(r, \theta = 0) \quad \Rightarrow \quad f_{21}(0) = f_{22}(0). \tag{42}$$

The eight differential equations together with the homogeneous boundary conditions and continuity conditions define a two-point boundary value problem. Solutions to the differential equations exist for certain values of s (eigenvalues). Because it has been impossible to determine s and integrate the governing differential equations analytically, a numerical approach has been taken by treating the problem as an initial value problem. A shooting method has been adopted whereby the differential equations in Layer 1 are integrated from their initial values at $\theta = \pi/2$ to $\theta = 0$. Likewise, the equations in Layer 2 are integrated from $\theta = -\pi/2$ to $\theta = 0$. This process is repeated systematically until the continuity conditions on the interface are satisfied within an acceptable level of accuracy. Since the eigenfunctions $f_{ij}(\theta)$ can only be determined to within a multiplicative constant, one can set $f_{11}(\pi/2) = 1$ without loss in generality. The quantities s, $f'_{11}(\pi/2)$, $f'_{12}(-\pi/2)$ and $f'_{22}(-\pi/2)$ are then treated as the primary unknowns. The numerical integration was performed using a fourth-order Runge–Kutta method. A Newton (secant) iterative scheme was employed to improve the "guesses" for the values of the unknowns. During the kth iteration the values of the unknowns are stored in a vector $\mathbf{x}^k$ as follows:

$$\mathbf{x}^k = \begin{bmatrix} x_1^k \\ x_2^k \\ x_3^k \\ x_4^k \end{bmatrix} = \begin{bmatrix} s \\ f'_{11}(\pi/2) \\ f'_{12}(-\pi/2) \\ f'_{22}(-\pi/2) \end{bmatrix}. \tag{43}$$

The errors in the satisfaction of the continuity conditions are stored in a vector $\mathbf{b}^k$ as follows:

$$\mathbf{b}^k = \begin{bmatrix} b_1^k \\ b_2^k \\ b_3^k \\ b_4^k \end{bmatrix} = \begin{bmatrix} f_{11}(x_1^k, x_2^k) - f_{12}(x_1^k, x_3^k, x_4^k) \\ f_{21}(x_1^k, x_2^k) - f_{22}(x_1^k, x_3^k, x_4^k) \\ E_1 f_{31}(x_1^k, x_2^k) - E_2 f_{32}(x_1^k, x_3^k, x_4^k) \\ E_1 f_{41}(x_1^k, x_2^k) - E_2 f_{42}(x_1^k, x_3^k, x_4^k) \end{bmatrix}. \tag{44}$$

The notation $f_{11}(x_1^k, x_2^k)$ is meant to indicate that the value of the function f_{11} on the interface ($\theta = 0$) in Layer 1 is a function of the unknowns x_1^k and x_2^k. The formula that produces a new estimate $(k+1)$ of the unknowns given sets of guesses at the kth and $(k-1)$th iterations is

$$\begin{bmatrix} x_1^{k+1} \\ x_2^{k+1} \\ x_3^{k+1} \\ x_4^{k+1} \end{bmatrix} = \begin{bmatrix} x_1^k \\ x_2^k \\ x_3^k \\ x_4^k \end{bmatrix} - \begin{bmatrix} k_{11} & k_{12} & k_{13} & k_{14} \\ k_{21} & k_{22} & k_{23} & k_{24} \\ k_{31} & k_{32} & k_{33} & k_{34} \\ k_{41} & k_{42} & k_{43} & k_{44} \end{bmatrix}^{-1} \begin{bmatrix} b_1^k \\ b_2^k \\ b_3^k \\ b_4^k \end{bmatrix}. \tag{45}$$

Explicit formulas for the terms in the "Jacobian" matrix are:

$$k_{i1} = \frac{[f_{i1}(x_1^{k-1}, x_2^{k-1}) - f_{i2}(x_1^{k-1}, x_3^{k-1}, x_4^{k-1})] - [f_{i1}(x_1^k, x_2^{k-1}) - f_{i2}(x_1^k, x_3^{k-1}, x_4^{k-1})]}{x_1^{k-1} - x_1^k} \tag{46}$$

$$k_{i2} = \frac{[f_{i1}(x_1^{k-1}, x_2^{k-1}) - f_{i2}(x_1^{k-1}, x_3^{k-1}, x_4^{k-1})] - [f_{i1}(x_1^{k-1}, x_2^k) - f_{i2}(x_1^{k-1}, x_3^{k-1}, x_4^{k-1})]}{x_2^{k-1} - x_2^k} \tag{47}$$

$$k_{i3} = \frac{[f_{i1}(x_1^{k-1}, x_2^{k-1}) - f_{i2}(x_1^{k-1}, x_3^{k-1}, x_4^{k-1})] - [f_{i1}(x_1^{k-1}, x_2^{k-1}) - f_{i2}(x_1^{k-1}, x_3^k, x_4^{k-1})]}{x_3^{k-1} - x_3^k} \tag{48}$$

$$k_{i4} = \frac{[f_{i1}(x_1^{k-1}, x_2^{k-1}) - f_{i2}(x_1^{k-1}, x_3^{k-1}, x_4^{k-1})] - [f_{i1}(x_1^{k-1}, x_2^{k-1}) - f_{i2}(x_1^{k-1}, x_3^{k-1}, x_4^k)]}{x_4^{k-1} - x_4^k}. \tag{49}$$

The subscript i takes on the values $i = 1, 2, 3, 4$. Note that when $i = 3$ or 4, the f_{i1} terms must be multiplied by E_1 and the f_{i2} terms must be multiplied by E_2, respectively [see eqns (39)–(40)].

NUMERICAL RESULTS

For potential practical application of the present theory, specific numerical results are presented for two material combinations that occur frequently in thin-film microelectronics, namely silicon–nitride/aluminum and silicon/aluminum. All results are for plane strain deformation. The material properties data were obtained from the references provided by Brady and Clauser (1986), Bleach and Meieran (1967) and Lynch (1975).

(i) *Silicon–nitride/aluminum* (Si_3N_4/Al)

$$E_1 = 70.6 \text{ GPa}, \quad \nu_1 = 0.345, \quad E_{T1} = \text{variable}$$

$$E_2 = 220.0 \text{ GPa}, \quad \nu_2 = 0.27, \quad E_{T2} = \text{variable}.$$

Table 1. Stress singularity for various stress–strain response combinations

(α_1, α_2)	Si_3N_4/Al	Si/Al
(1.0,1.0)	$r^{-0.10244}$	$r^{-0.06933}$
(0.5,0.5)	$r^{-0.12536}$	$r^{-0.08674}$
(0.0,0.0)	$r^{-0.15331}$	$r^{-0.10818}$
(0.5,1.0)	$r^{-0.21559}$	$r^{-0.18519}$
(0.0,0.5)	$r^{-0.40530}$	$r^{-0.40526}$
(0.0,1.0)	$r^{-0.40534}$	$r^{-0.40533}$
(1.0,0.0)	$r^{-0.40461}$	$r^{-0.40479}$

(ii) *Silicon/aluminum* (Si/Al)

$$E_1 = 70.6 \text{ GPa}, \quad \nu_1 = 0.345, \quad E_{T1} = \text{variable}$$
$$E_2 = 170.0 \text{ GPa}, \quad \nu_2 = 0.28, \quad E_{T2} = \text{variable}.$$

Convergence of the current analysis was considered adequate when $|f_{11}(0) - f_{12}(0)| < 10^{-4}$, $|f_{21}(0) - f_{22}(0)| < 10^{-4}$, $|E_1 f_{31}(0) - E_2 f_{32}(0)| < 10^{-4}$ and $|E_1 f_{41}(0) - E_2 f_{42}(0)| < 10^{-4}$. Convergence was typically obtained in less than 10 iterations. Since the material model selected is not valid when $\alpha \to 0$, results reported here for $\alpha = 0$ are actually limiting values using $\alpha = 1 \times 10^{-5}$. Flow theory plasticity must be used to obtain rigorous results for this situation.

For the special case where the materials are linear elastic ($\alpha_1 = \alpha_2 = 1$), the stress singularity for Si_3N_4/Al is $r^{-0.10244}$, while the stress singularity for Si/Al is $r^{-0.06933}$. These results are in complete agreement with the often quoted results of Bogy (1970). Values of r^{s-1} for various combinations of α_1 and α_2 are given in Table 1. For linear elastic materials ($\alpha_1 = \alpha_2 = 1$), the degree of singularity is always smaller than that for bilinear materials ($\alpha_1, \alpha_2 \neq 1$). The strongest singularity occurs when one layer is linear elastic and the other layer is nearly elastic–perfectly-plastic. Angular dependence of the eigenfunctions for the Si_3N_4/Al material combination when $\alpha_1 = 0.5$, $\alpha_2 = 1.0$ is shown in Fig. 2. Inspection of

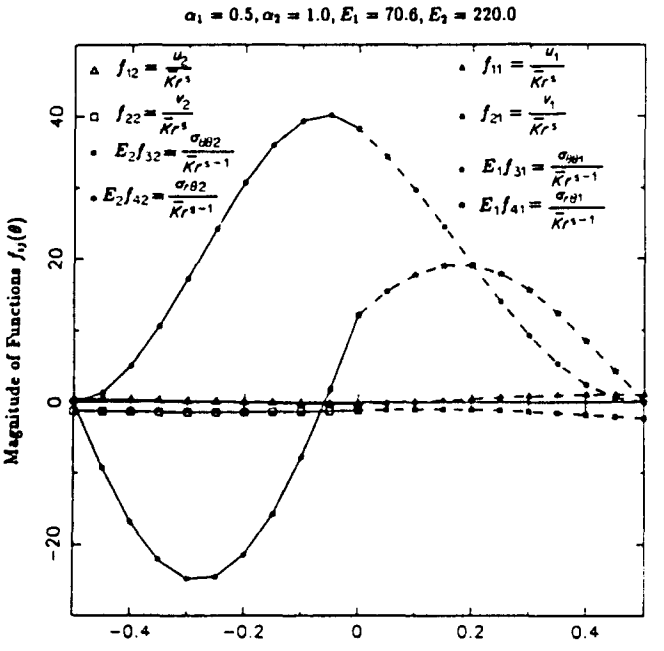

Fig. 2. Angular dependence of the eigenfunctions for Si_3N_4/Al.

Table 2. Stress singularity for various E_2/E_1 ratios

(α_1, α_2)	$\frac{E_2}{E_1}$	ν_1	ν_2	Singularity
(1.0,1.0)	2.0	0.345	0.27	$r^{-0.04977}$
(1.0,1.0)	5.0	0.345	0.27	$r^{-0.15901}$
(1.0,1.0)	10.0	0.345	0.27	$r^{-0.22327}$
(1.0,1.0)	20.0	0.345	0.27	$r^{-0.26541}$
(0.5,0.5)	2.0	0.345	0.27	$r^{-0.06050}$
(0.5,0.5)	5.0	0.345	0.27	$r^{-0.19061}$
(0.5,0.5)	10.0	0.345	0.27	$r^{-0.26356}$
(0.5,0.5)	20.0	0.345	0.27	$r^{-0.36911}$
(0.0,0.0)	2.0	0.345	0.27	$r^{-0.07548}$
(0.0,0.0)	5.0	0.345	0.27	$r^{-0.22681}$
(0.0,0.0)	10.0	0.345	0.27	$r^{-0.30476}$
(0.0,0.0)	20.0	0.345	0.27	$r^{-0.35156}$

Table 3. Stress singularity for various Poisson's ratios (ν_1, ν_2) (linear materials)

(α_1, α_2)	$\frac{E_2}{E_1}$	ν_1	ν_2	Singularity
(1.0,1.0)	3.1	0.345	0.27	$r^{-0.10244}$
(1.0,1.0)	3.1	0.345	0.30	$r^{-0.10097}$
(1.0,1.0)	3.1	0.345	0.33	$r^{-0.09940}$
(1.0,1.0)	3.1	0.345	0.36	$r^{-0.09774}$
(1.0,1.0)	3.1	0.33	0.27	$r^{-0.09721}$
(1.0,1.0)	3.1	0.30	0.27	$r^{-0.08631}$
(1.0,1.0)	3.1	0.27	0.27	$r^{-0.07485}$

Table 4. Stress singularity for various Poisson's ratios (ν_1, ν_2) (bilinear materials)

(α_1, α_2)	$\frac{E_2}{E_1}$	ν_1	ν_2	Singularity
(0.5,0.5)	3.1	0.345	0.27	$r^{-0.12536}$
(0.5,0.5)	3.1	0.345	0.30	$r^{-0.12519}$
(0.5,0.5)	3.1	0.345	0.33	$r^{-0.12500}$
(0.5,0.5)	3.1	0.345	0.36	$r^{-0.12481}$
(0.5,0.5)	3.1	0.33	0.27	$r^{-0.12277}$
(0.5,0.5)	3.1	0.30	0.27	$r^{-0.11746}$
(0.5,0.5)	3.1	0.27	0.27	$r^{-0.11193}$
(0.0,0.0)	3.1	0.345	0.27	$r^{-0.15329}$
(0.0,0.0)	3.1	0.345	0.30	$r^{-0.15329}$
(0.0,0.0)	3.1	0.345	0.33	$r^{-0.15329}$
(0.0,0.0)	3.1	0.345	0.36	$r^{-0.15329}$
(0.0,0.0)	3.1	0.33	0.27	$r^{-0.15329}$
(0.0,0.0)	3.1	0.30	0.27	$r^{-0.15329}$
(0.0,0.0)	3.1	0.27	0.27	$r^{-0.15329}$

this figure reveals that the continuity of displacement and traction on the interface is satisfied along with traction-free conditions on the free edge.

Table 2 shows the dependence of the strength of the singularity on the ratio E_2/E_1, holding Poisson's ratio constant. The singularity increases as the ratio E_2/E_1 increases.

Table 3 shows the relatively weak dependence of the stress singularity on the values of ν_1 and ν_2 for linear materials, holding the ratio of E_2/E_1 constant. The results show that the degree of singularity remains relatively small for widely varying values of Poisson's ratio.

Table 4 shows the dependence of the stress singularity on various values of ν_1 and ν_2, for bilinear materials. Again, Poisson's ratio has a relatively weak influence on the stress singularity.

CONCLUSIONS

The stress singularity r^{s-1} for $0 < s \leqslant 1$ that occurs at the free edge in a bimaterial strip with bilinear material properties has been investigated. The singularity is typically much stronger when the materials exhibit a bilinear stress–strain response, compared with linear elastic materials.

Acknowledgement—Financial support for this work was provided by the National Science Foundation through Grant MSM-8708980 to North Carolina State University.

REFERENCES

Bleach, I. A. and Meieran, E. S. (1967). Enhanced X-ray diffraction from substrate crystals containing discontinuous surface films. *J. Appl. Phys.* **38**, 2913–2919.

Bogy, D. B. (1968). Edge-bonded dissimilar orthogonal elastic wedges under normal and shear loading. *J. Appl. Mech.* **35**, 460–466.

Bogy, D. B. (1970). On the problem of edge-bonded elastic quarter planes loaded at the boundary. *Int. J. Solids Structures* **6**, 1287–1313.

Bogy, D. B. (1971). Two edge-bonded elastic wedges of different materials and wedge angles under surface tractions. *J. Appl. Mech.* **38**, 377–386.

Brady, G. S. and Clauser, H. R. (1986). *Materials Handbook*, 12th edn, p. 723. McGraw-Hill, Maidenhead, U.K.

Dempsey, J. P. and Sinclair, G. B. (1981). On the singular stress behavior at the vertices of bimaterial wedge. *J. Elasticity*. **11**(3), 317–327.

Dundurs, J. (1969). Discussion of edge-bonded dissimilar orthogonal elastic wedges under normal and shear loading. *J. Appl. Mech.* **36**, 650–652.

Duva, J. M. (1988). The singularity at the apex of a rigid wedge embedded in a nonlinear material. *J. Appl. Mech.* **55**, 361–364.

Hein, V. L. and Erdogan, F. (1971). Stress singularities in a two material wedge. *Int. J. Fract. Mech.* **7**(7), 317–330.

Hutchinson, J. W. (1968). Singular behavior at the end of a tensile crack in a hardening material. *J. Mech. Phys. Solids* **16**, 13–31.

Lynch, C. T. (1975). *Handbook of Materials Science*, Vol. II, p. 178. CRC Press, Boca Raton, FL.

Ponte Castañeda, P. (1987). Asymptotic fields in steady crack growth with linear strain hardening. *J. Mech. Phys. Solids*. **35**, 227–268.